

TIME DELAY ESTIMATION FROM MULTIBAND RADIO CHANNEL SAMPLES IN NONUNIFORM NOISE

Tarik Kazaz, Gerard J. M. Janssen and Alle-Jan van der Veen

Faculty of EEMCS, Delft University of Technology, Delft, The Netherlands

ABSTRACT

The multipath radio channel is considered to have a non-bandlimited channel impulse response. Therefore, it is challenging to achieve high resolution time-delay (TD) estimation of multipath components (MPCs) from bandlimited observations of communication signals. In this paper, we consider the problem of multiband channel sampling and TD estimation of MPCs. We assume that the nonideal multi-branch receiver is used for multiband sampling, where the noise is nonuniform across the receiver branches. The resulting data model of Hankel matrices formed from acquired samples has multiple shift-invariance structures, and we propose an algorithm for TD estimation using weighted subspace fitting. The subspace fitting is formulated as a separable nonlinear least squares (NLS) problem, and it is solved using a variable projection method. The proposed algorithm supports high resolution TD estimation from an arbitrary number of bands, and it allows for nonuniform noise across the bands. Numerical simulations show that the algorithm almost attains the Cramér Rao Lower Bound, and it outperforms previously proposed methods such as multiresolution TOA, MI-MUSIC, and ESPRIT.

Index Terms— time-of-arrival, channel estimation, super-resolution, sparse recovery, multiband sampling, cognitive radio

1. INTRODUCTION

The first step of time-delay (TD) estimation is an estimation of the multipath components of the underlying communication channel. Since the impulse response of multipath radio channels is considered to be not bandlimited, it is challenging to achieve high resolution TD estimation from bandlimited observations of communications signals. Traditional channel modeling is mainly suited for communication system design, where it is more important to estimate the effects of the channel on the signal to perform equalization, rather than estimating the parameters of the underlying multipath channel. Therefore, radio channels are typically modeled as FIR filters where the time resolution of the channel is inversely proportional to the bandwidth of the signal used for channel probing [1].

Therefore, high resolution channel estimation requires modeling assumptions. Modeling the channel impulse response (CIR) as a sparse sequence of Diracs, time-delay estimation becomes a problem of parametric spectral inference from observed bandlimited signals. Under this assumption, theoretically, it is possible to obtain perfect estimates of the channel parameters from an equally finite number of samples taken in the frequency domain [2].

Many algorithms for TD estimation from frequency domain samples have been proposed in the past. These algorithms are usually based on (i) subspace estimation [3, 4, 5, 6], (ii) finite rate of innovation [2, 7, 8], or (iii) compressed sampling [9, 10, 11, 12, 13, 14] methods. Few of the previous works [8, 10, 11, 14] discuss issues related to frequency domain sampling. However, these methods are typically complex for the implementation or not robust to noise.

The resolution of TD estimation is proportional to the frequency aperture of the samples taken in the frequency domain. To improve the resolution of TD estimation, without arriving at unrealistic sampling rates, multiband channel sampling has been proposed in [15]. In [16] a practical multibranch receiver for multiband channel sampling has been proposed. Due to hardware impairments of analog electronics components such as low-noise and power amplifiers, the noise level is typically varying across the receiver branches.

In this paper, we are interested in a generalized algorithm for high resolution TD estimation from an arbitrary number of sampled bands with nonuniform noise. Following the shift-invariance structure of Hankel matrices formed from the acquired samples, we propose an algorithm for TD estimation based on weighted subspace fitting [17, 18]. We formulate weighted subspace fitting as a separable nonlinear least squares problem and solve it using the variable projection method [19]. To initialize the variable projection method, we use the TD estimate obtained via the multiresolution TOA algorithm [16]. With this initialization, the iteration of the variable projection method converges very fast, typically within three steps for moderate or high signal-to-noise ratios (SNR).

The resulting algorithm is benchmarked through simulations by comparing its performance with the algorithms proposed in [20, 21, 16] and the Cramér Rao Lower Bound (CRLB). The results show that for low SNR, the proposed algorithm provides better performance than previously proposed algorithms, and it almost attains the CRLB.

2. PROBLEM FORMULATION

Consider a multipath radio channel model with K propagation paths defined by a continuous-time impulse and frequency response as

$$h(t) = \sum_{k=1}^K \alpha_k \delta(t - \tau_k) \quad \text{and} \quad H(\omega) = \sum_{k=1}^K \alpha_k e^{-j\omega\tau_k}, \quad (1)$$

where $\alpha = [\alpha_1, \dots, \alpha_K]^T \in \mathbb{C}^K$ and $\tau = [\tau_1, \dots, \tau_K]^T \in \mathbb{R}_+^K$ are collecting unknown gains and time-delays of the MPCs, respectively [22]. We are interested in estimating α and τ by probing the channel using the known wideband probing signal $s_i(t)$ transmitted over $i = 0, \dots, L - 1$, separate frequency bands (cf. Fig. 1a). The probed frequency bands are $\mathcal{W}_i = [\omega_i - \frac{B}{2}, \omega_i + \frac{B}{2}]$, where B is the bandwidth, and ω_i is the central angular frequency of the i th

This research was supported in part by NWO-STW under contract 13970 (“SuperGPS”).

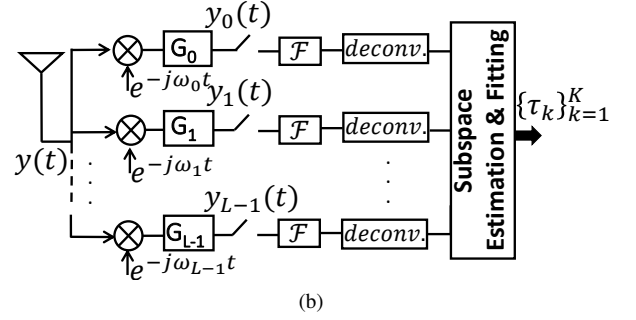
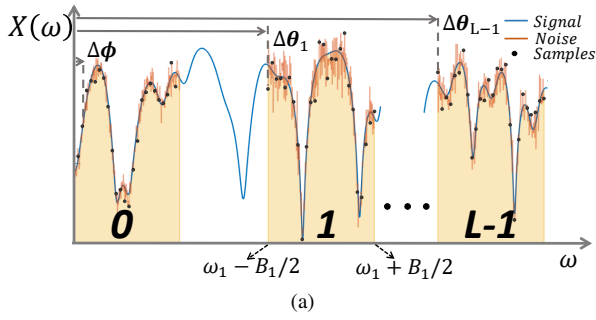


Fig. 1: (a) The multiband channel frequency response, and (b) a multibranch receiver with L RF chains.

band. We consider that measurements are collected using nonideal multibranch transceivers with nonuniform noise across the receiver branches. Our objective is to estimate τ from an arbitrary number of sampled bands while considering the difference in noise levels of the acquired samples.

3. DATA MODEL

Continuous-time signal model: We consider a baseband signal model and assume ideal conversion to and from the passband without phase and synchronization errors. The response of RF chains at the probed frequency bands are modeled using equivalent linear and time-invariant low-pass filters $g_i(t)$, where the corresponding CTFT $G_i(\omega)$ has passband $[-\frac{B}{2}, \frac{B}{2}]$ (cf. Fig. 1b). We assume that the frequency responses of the RF chains $G_i(\omega)$ are characterized during calibration and known. The algorithm for time-delay estimation in the case when $G_i(\omega)$, $i = 0, \dots, L-1$, are unknown is proposed in [23]. The impulse response of the i th channel band is $h_i(t)$, and its CTFT is $H_i(\omega) = H(\omega_i + \omega)$. Assume that $h_i(t)$ is time-limited.

Consider that the same probing signal is transmitted in all bands, that is, $s_i(t) = s(t)$ and $B_i = B$ for $i = 0, \dots, L-1$. The signal received at the i th band after conversion to the baseband and low-pass filtering is

$$y_i(t) = s(t) * g_i(t) * h_i(t) + q_i(t), \quad (2)$$

where $q_i(t)$ is low-pass filtered Gaussian white noise. The corresponding CTFT of the signal $y_i(t)$ is

$$Y_i(\omega) = \begin{cases} S(\omega)G_i(\omega)H_i(\omega) + Q_i(\omega), & \omega \in [-\frac{B}{2}, \frac{B}{2}] \\ 0, & \text{otherwise,} \end{cases} \quad (3)$$

where $S(\omega)$ and $Q_i(\omega)$ are the CTFTs of $s(t)$ and $q_i(t)$, respectively.

Discrete-time signal model: The receiver samples $y_i(t)$ with period $T_s = 1/B$, performs packet detection and frequency synchronization. During the period of single probing signal, N complex samples are collected and $T_{sym} = NT_s$. Next, N -point DFT is applied on the collected samples, and they are stacked in increasing order of the DFT frequencies in $\mathbf{y}_i \in \mathbb{C}^N$. Then, the discrete data model of the received signal (3) can be written as

$$\mathbf{y}_i = \text{diag}(\mathbf{s} \circ \mathbf{g}_i) \mathbf{h}_i + \mathbf{q}_i, \quad (4)$$

where \circ is the Khatri-Rao product, \mathbf{s} collects the known symbols, \mathbf{g}_i , and \mathbf{q}_i , collect samples of $G_i(\omega)$, and $Q_i(\omega)$ at the sampling

frequencies, respectively. Likewise, $\mathbf{h}_i \in \mathbb{C}^N$ collects samples of $H_i(\omega)$ as

$$H_i[n] = H(\omega_i + n\omega_s), \quad n = -\frac{N}{2}, \dots, \frac{N}{2}, \quad (5)$$

where $\omega_s = \frac{2\pi}{NT_s}$, and we assume that N is an even number. We consider that bands $\{\mathcal{W}_i\}_{i=0}^{L-1}$ are laying on the discrete frequency grid $\omega_i = \omega_0 + n_i\omega_s$, where $n_i \in \mathbb{N}$, and ω_0 denotes the lowest frequency considered during channel probing. Inserting the channel model (1) into (5) gives

$$H_i[n] = \sum_{k=1}^K \alpha_k e^{-jn_i\omega_s\tau_k} e^{-jn\omega_s\tau_k}, \quad (6)$$

where we absorbed $e^{-j\omega_0\tau_k}$ in $\alpha_k \forall k$. Now, the channel vector \mathbf{h}_i satisfies the model

$$\mathbf{h}_i = \mathbf{M} \text{diag}(\boldsymbol{\theta}_i) \boldsymbol{\alpha}, \quad (7)$$

where $\mathbf{M} \in \mathbb{C}^{N \times K}$ is a Vandermonde matrix

$$\mathbf{M} = \begin{bmatrix} 1 & 1 & \dots & 1 \\ \Phi_1 & \Phi_2 & \dots & \Phi_K \\ \vdots & \vdots & \ddots & \vdots \\ \Phi_1^{N-1} & \Phi_2^{N-1} & \dots & \Phi_K^{N-1} \end{bmatrix}, \quad (8)$$

and $\Phi_k = e^{-j\phi_k}$, where $\phi_k = \omega_s\tau_k$. Likewise, the band dependent phase shifts of MPCs are collected in $\boldsymbol{\theta}_i = [\theta_{i,1}, \dots, \theta_{i,K}]^T \in \mathbb{C}^K$, where $\theta_{i,k} = \Phi_k^{n_i}$.

Next, we assume that none of the entries of \mathbf{s} or \mathbf{g}_i are zero or close to zero, and estimate \mathbf{h}_i by applying deconvolution on the data vector (4) as

$$\mathbf{h}_i = \text{diag}^{-1}(\mathbf{s} \circ \mathbf{g}_i) \mathbf{y}_i,$$

which satisfies the model

$$\mathbf{h}_i = \mathbf{M} \boldsymbol{\Theta}_i \boldsymbol{\alpha} + \mathbf{q}'_i. \quad (9)$$

where $\boldsymbol{\Theta}_i = \text{diag}(\boldsymbol{\theta}_i)$. The symbols \mathbf{s} have the constant magnitude, and we assume that frequency responses of receiver chains \mathbf{g}_i are almost flat. Therefore $\mathbf{q}'_i = \text{diag}^{-1}(\mathbf{s} \circ \mathbf{g}_i) \mathbf{q}_i$ is a zero-mean white Gaussian distributed noise with covariance $\boldsymbol{\Sigma}_i = \sigma_i^2 \mathbf{I}_N$, where \mathbf{I}_N is the $N \times N$ identity matrix. In the case that the frequency responses of the RF chains are not perfectly flat, \mathbf{q}'_i will be colored noise. However, its coloring is known and can be taken into account.

4. MULTIBAND TIME-DELAY ESTIMATION

Our next objective is to estimate τ from the channel estimates \mathbf{h}_i , $i = 0, \dots, L-1$. We begin by stacking the channel estimates in the multiband channel vector $\mathbf{h} = [\mathbf{h}_0^T, \dots, \mathbf{h}_{L-1}^T]^T \in \mathbb{C}^{NL}$. From (9), \mathbf{h} satisfies the model

$$\mathbf{h} = \mathbf{A}(\tau)\boldsymbol{\alpha} + \mathbf{q} := \begin{bmatrix} \mathbf{M} \\ \mathbf{M}\boldsymbol{\Theta}_1 \\ \vdots \\ \mathbf{M}\boldsymbol{\Theta}_{L-1} \end{bmatrix} \boldsymbol{\alpha} + \begin{bmatrix} \mathbf{q}'_0 \\ \mathbf{q}'_1 \\ \vdots \\ \mathbf{q}'_{L-1} \end{bmatrix}. \quad (10)$$

Since $\mathbf{A}(\tau)$ has a multiple shift-invariance structure and (10) resembles the data model of Multiple Invariance ESPRIT [18], τ can be estimated using a subspace fitting methods.

4.1. Multiband estimation algorithm

From the vectors \mathbf{h}_i , $i = 0, \dots, L-1$, we construct Hankel matrices of size $P \times Q$ as

$$\mathbf{H}_i = \begin{bmatrix} H_i[0] & H_i[1] & \cdots & H_i[Q] \\ H_i[1] & H_i[2] & \cdots & H_i[Q+1] \\ \vdots & \vdots & \ddots & \vdots \\ H_i[P-1] & H_i[P] & \cdots & H_i[N-1] \end{bmatrix}. \quad (11)$$

Here, $P = N - Q - 1$, Q is a design parameter and we require $P > K$ and $Q \geq K$. From (9), and using the shift invariance of the Vandermonde matrix (8), the constructed Hankel matrices satisfy

$$\mathbf{H}_i = \mathbf{M}'\boldsymbol{\Theta}_i\mathbf{X} + \mathbf{Q}_i, \quad (12)$$

where \mathbf{M}' is an $P \times K$ submatrix of \mathbf{M} ,

$$\mathbf{X} = [\boldsymbol{\alpha}, \boldsymbol{\Phi}\boldsymbol{\alpha}, \boldsymbol{\Phi}^2\boldsymbol{\alpha}, \dots, \boldsymbol{\Phi}^{Q-1}\boldsymbol{\alpha}],$$

\mathbf{Q}_i is a noise matrix, and $\boldsymbol{\Phi} = \text{diag}([\Phi_1 \cdots \Phi_K])$.

The column subspaces of \mathbf{H}_i , $i = 0, \dots, L-1$, are spanned by the same K dimensional basis. Therefore, a good initial estimate of the orthonormal basis that spans the column subspace of \mathbf{H}_i , $i = 0, \dots, L-1$, can be obtained from the low-rank approximation of the block Hankel matrix

$$\mathbf{H}_r = [\mathbf{H}_0 \quad \mathbf{H}_1 \quad \cdots \quad \mathbf{H}_{L-1}]. \quad (13)$$

The matrix \mathbf{H}_r satisfies the model

$$\mathbf{H}_r = \mathbf{M}'\mathbf{X}_r + \mathbf{Q}_r,$$

where $\mathbf{X}_r = [\mathbf{X}, \boldsymbol{\Theta}_1\mathbf{X}, \dots, \boldsymbol{\Theta}_{L-1}\mathbf{X}]$, and likewise $\mathbf{Q}_r = [\mathbf{Q}_0, \dots, \mathbf{Q}_{L-1}]$. Let \mathbf{U}_r be a K dimensional orthonormal basis for the column span of \mathbf{H}_r , then $\mathbf{P}_{\mathbf{U}_r} = \mathbf{U}_r\mathbf{U}_r^H$ is the corresponding projection matrix. To perform noise reduction, we project \mathbf{H}_i , $i = 0, \dots, L-1$, onto the column subspace of \mathbf{U}_r and form the block Hankel matrix

$$\mathbf{H} = (\mathbf{I}_L \otimes \mathbf{P}_{\mathbf{U}_r}) \begin{bmatrix} \mathbf{H}_0 \\ \mathbf{H}_1 \\ \vdots \\ \mathbf{H}_{L-1} \end{bmatrix},$$

where \otimes is the Kronecker product. Now, \mathbf{H} satisfies the model

$$\mathbf{H} = \mathbf{A}'(\tau)\mathbf{X} + \mathbf{Q} := \begin{bmatrix} \mathbf{M}' \\ \mathbf{M}'\boldsymbol{\Theta}_1 \\ \vdots \\ \mathbf{M}'\boldsymbol{\Theta}_{L-1} \end{bmatrix} \mathbf{X} + \begin{bmatrix} \mathbf{P}_{\mathbf{U}_r}\mathbf{Q}_0 \\ \mathbf{P}_{\mathbf{U}_r}\mathbf{Q}_1 \\ \vdots \\ \mathbf{P}_{\mathbf{U}_r}\mathbf{Q}_{L-1} \end{bmatrix}. \quad (14)$$

Note that $\mathbf{A}'(\tau)$ has multiple shift-invariance structures introduced by the phase shifts of τ on the (i) sampling frequency, $\boldsymbol{\Phi}$, and (ii) carrier frequencies of the bands, $\boldsymbol{\Theta}_i = \boldsymbol{\Phi}^{n_i}$, $i = 0, \dots, L-1$, as shown in Fig. 1a. The phase shifts $\boldsymbol{\Phi}$ can be estimated from the low-rank approximation of \mathbf{H} and its shift-invariance properties using subspace fitting methods. From the estimate of $\boldsymbol{\Phi}$, τ immediately follows.

Let \mathbf{U} be a K -dimensional orthonormal basis for the column span of \mathbf{H} , obtained using the singular value decomposition [24], then we can write $\mathbf{A}'(\tau) = \mathbf{U}\mathbf{T}$, where \mathbf{T} is a $K \times K$ nonsingular matrix. Next, let us define selection matrices

$$\begin{aligned} \mathbf{J}_{i,1} &= \mathbf{e}_i^T \otimes [\mathbf{I}_{P-1} \quad \mathbf{0}_{P-1}], \\ \mathbf{J}_{i,2} &= \mathbf{e}_i^T \otimes [\mathbf{0}_{P-1} \quad \mathbf{I}_{P-1}], \end{aligned} \quad (15)$$

where $(\cdot)^T$ is transpose, $\mathbf{0}_{P-1}$ is a zero vector of size $P-1$, \mathbf{e}_i is a vector of size L , with i th element equal to 1 and zero otherwise. To estimate $\boldsymbol{\Phi}$ we select submatrices consisting of the first and, respectively, the last row of each block matrix stacked in \mathbf{U} , that is $\mathbf{U}_{i,1} = \mathbf{J}_{i,1}\mathbf{U}$ and $\mathbf{U}_{i,2} = \mathbf{J}_{i,2}\mathbf{U}$, $i = 0, \dots, L-1$. In the view of shift-invariance structure of $\mathbf{A}'(\tau)$, we have

$$\mathbf{U}_{i,1} = \mathbf{M}''\boldsymbol{\Phi}^{n_i}, \quad \mathbf{U}_{i,2} = \mathbf{M}''\boldsymbol{\Phi}^{n_i+1}, \quad (16)$$

where \mathbf{M}'' is a $(P-1) \times K$ submatrix of \mathbf{M}' . Next, we form block matrices

$$\boldsymbol{\mathcal{U}} = \begin{bmatrix} \mathbf{U}_{0,1} \\ \mathbf{U}_{0,2} \\ \vdots \\ \mathbf{U}_{L-1,2} \end{bmatrix}, \quad \boldsymbol{\mathcal{A}} = \begin{bmatrix} \mathbf{M}'' \\ \mathbf{M}''\boldsymbol{\Phi} \\ \vdots \\ \mathbf{M}''\boldsymbol{\Phi}^{n_{L-1}+1} \end{bmatrix}. \quad (17)$$

Finally, $\boldsymbol{\Phi}$ can be estimated by solving the following weighted subspace fitting problem

$$\begin{aligned} \hat{\boldsymbol{\Phi}} &= \underset{\boldsymbol{\Phi}}{\text{argmin}} \left\| \mathbf{W}^{1/2} (\boldsymbol{\mathcal{U}} - \boldsymbol{\mathcal{A}}\mathbf{T}^{-1}) \right\|_F^2 \\ &= \underset{\boldsymbol{\Phi}}{\text{argmin}} \left\| \mathbf{W}^{1/2} (\mathbf{I} - \mathbf{P}_{\boldsymbol{\mathcal{A}}(\boldsymbol{\Phi}))} \boldsymbol{\mathcal{U}} \right\|_F^2 \end{aligned} \quad (18)$$

where $\mathbf{P}_{\boldsymbol{\mathcal{A}}(\boldsymbol{\Phi})} = \boldsymbol{\mathcal{A}}\boldsymbol{\mathcal{A}}^\dagger$, $(\cdot)^\dagger$ is the pseudoinverse of a matrix, and $\mathbf{W} = \mathbf{I}_{2L(P-1)}$ for the case when noise is uniform across the receiver chains branches. When the noise power is nonuniform across the receiver branches, the weighting matrix is given by $\mathbf{W} = \text{blkdiag}(\boldsymbol{\Sigma}'_0, \dots, \boldsymbol{\Sigma}'_{L-1}) \in \mathbb{C}^{2L(P-1) \times 2L(P-1)}$, where $\boldsymbol{\Sigma}'_i = \sigma_i^2 \mathbf{I}_{P-1}$ and we assume that σ_i , $i = 0, \dots, L-1$, are known.

The subspace fitting problem (18) can be formulated as a separable nonlinear least squares problem, which can be solved efficiently using several iterative optimization methods (e.g., variable projection, Gauss-Newton or Levenberg-Marquardt). We use the variable projection method [19] to find a solution, where a good initialization

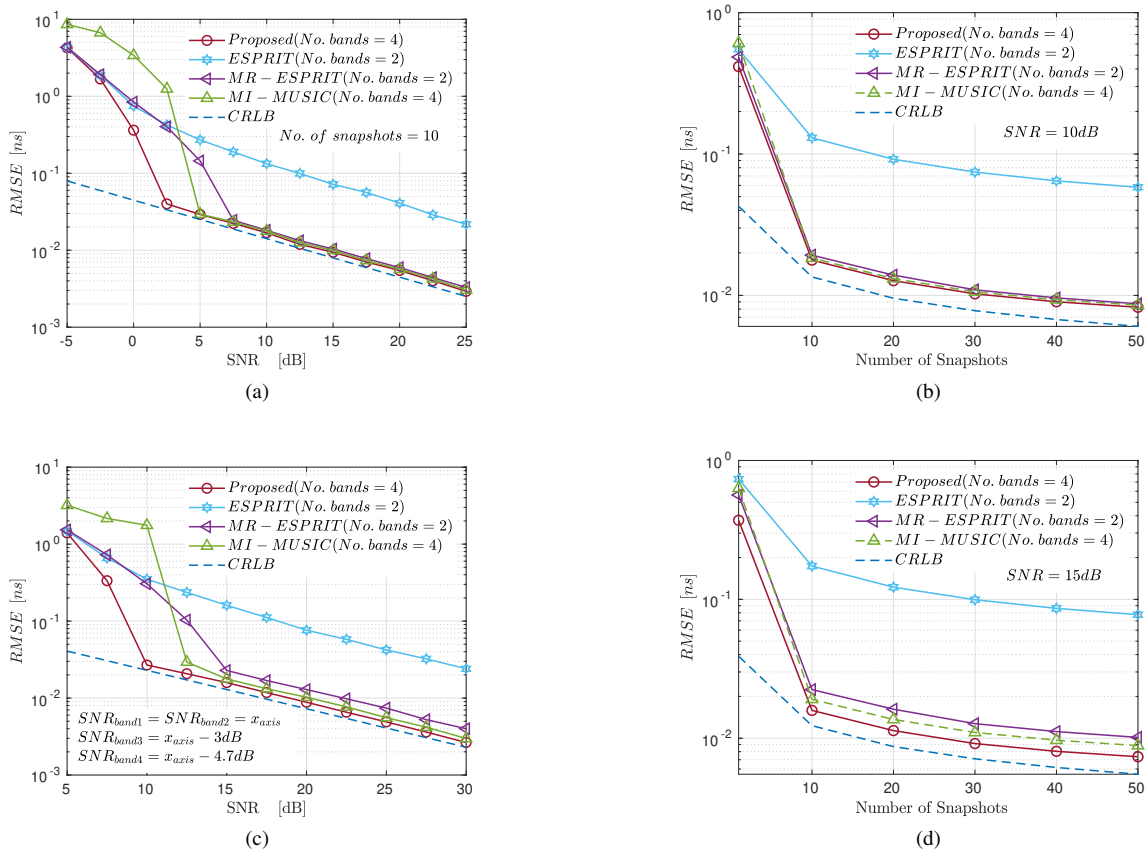


Fig. 2: RMSE for estimated time-delay in uniform (a-b) and nonuniform noise (c-d) vs signal to noise ratio and number of snapshots.

is obtained by the multiresolution TOA algorithm [16]. With this initialization, the variable projection method converges very fast, typically within three steps for moderate and high signal-to-noise ratios (SNR).

5. NUMERICAL EXPERIMENTS

This section evaluates the performance of the proposed algorithm via numerical simulations. We consider a scenario where the multipath channel has nine dominant MPCs, i.e., $K = 9$, with gain of line-of-sight (LOS) MPC distributed according to a Rician distribution. The continuous-time channel is modeled using a 2 GHz grid, with channel tap delays spaced at 500 ps. We consider that the receiver estimates the channel frequency response in four frequency bands, i.e., $L = 4$, using probing signal with bandwidth of $B = 80$ MHz. The central frequencies of the bands are $\{60, 180, 290, 400\}$ MHz, respectively. To evaluate the performance of TD estimation, we use the root mean square error (RMSE) of the LOS multipath component TD estimate. The RMSEs are computed using 10^3 independent Monte-Carlo trials and compared with the CRLB and RMSEs of the algorithms proposed in [16, 20, 21] which are shortly denoted with MR-ESPRIT, ESPRIT, and MI-MUSIC, respectively.

Fig. 2a shows the performance of the proposed, MR-ESPRIT, ESPRIT, and MI-MUSIC algorithms in different signal-to-noise ratio (SNR) regimes for the case when noise power is uniform across

the receiver branches. The number of channel snapshots is set to 10 and kept fixed during trials. From Fig. 2a, we observe that the RMSE of TD estimation decreases with SNR. The MR-ESPRIT and ESPRIT algorithms utilize only samples available from the first and fourth band. Therefore, as expected, their performance is worse, compared to the performance of the proposed and MI-MUSIC algorithms. The MR-ESPRIT, MI-MUSIC and the proposed algorithms are all almost attaining the CRLB for sufficiently high SNR, while ESPRIT due to inefficient use of available data is not able to resolve closely spaced MPCs even for high SNR. The proposed algorithm attains the CRLB for lower SNR than any of the algorithms used for comparison.

In the second scenario, we fixed the signal-to-noise ratio to $SNR = 10$ dB and evaluated the performance of algorithms for the different number of snapshots. From Fig. 2b, it is seen that the RMSE of TD estimation decreases with the number of snapshots. It can be observed that the number of snapshots needs to be sufficiently high, i.e., equal or higher than 10, for the algorithms to perform well, which is the consequence of the errors introduced by signal subspace estimation.

The same simulation scenarios are repeated for the case when the noise power is nonuniform across the receiver branches, and the corresponding RMSEs are shown in Fig. 2c and Fig. 2d. The signal-to-noise ratios in the third and fourth band are set to -3 dB and -4.7 dB compared to the SNR of the x-axis on the Fig.2c. Likewise, in the fourth scenario, the signal-to-noise ratios for the third and fourth

bands are set to 12 dB and 11.3 dB, respectively. Due to the appropriate weighting of the cost function (18), the proposed algorithm is still close to the CRLB also in the case of nonuniform noise.

6. CONCLUSIONS

In this paper, we proposed an algorithm for time-delay estimation from multiband channel measurements. Considering the channel impulse response as a sparse signal in the time domain, we have formulated time-delay estimation as a problem of parametric spectral inference from observed multiband measurements. The acquired measurements exhibit multiple shift-invariance structures, and we estimate time-delays by solving the subspace fitting problem. The solution to the problem is found efficiently using the variable projection method. Future directions aim towards evaluating the proposed algorithm with real channel measurements and solving the problem of joint time-delay estimation and calibration of RF chains.

7. REFERENCES

- [1] K. Witrisal *et al.*, “Noncoherent ultra-wideband systems,” *IEEE Signal Processing Magazine*, vol. 26, no. 4, 2009.
- [2] M. Vetterli, P. Marziliano, and T. Blu, “Sampling signals with finite rate of innovation,” *IEEE transactions on Signal Processing*, vol. 50, no. 6, pp. 1417–1428, 2002.
- [3] A.-J. Van der Veen, M. C. Vanderveen, and A. Paulraj, “Joint angle and delay estimation using shift-invariance techniques,” *IEEE Transactions on Signal Processing*, vol. 46, no. 2, pp. 405–418, 1998.
- [4] X. Li and K. Pahlavan, “Super-resolution TOA estimation with diversity for indoor geolocation,” *IEEE Transactions on Wireless Communications*, vol. 3, no. 1, pp. 224–234, 2004.
- [5] M. Pourkhaatoun and S. A. Zekavat, “High-resolution low-complexity cognitive-radio-based multiband range estimation: Concatenated spectrum vs. Fusion-based,” *IEEE Systems Journal*, vol. 8, no. 1, pp. 83–92, 2014.
- [6] T. Kazaz *et al.*, “Joint ranging and clock synchronization for dense heterogeneous iot networks,” in *2018 52nd Asilomar Conference on Signals, Systems, and Computers*. IEEE, 2018, pp. 2169–2173.
- [7] I. Maravic, J. Kusuma, and M. Vetterli, “Low-sampling rate UWB channel characterization and synchronization,” *Journal of Communications and Networks*, vol. 5, no. 4, pp. 319–327, Dec 2003.
- [8] I. Maravic and M. Vetterli, “Sampling and reconstruction of signals with finite rate of innovation in the presence of noise,” *IEEE Transactions on Signal Processing*, vol. 53, no. 8, pp. 2788–2805, 2005.
- [9] K. M. Cohen *et al.*, “Channel estimation in UWB channels using compressed sensing,” in *Acoustics, Speech and Signal Processing (ICASSP), 2014 IEEE International Conference on*. IEEE, 2014, pp. 1966–1970.
- [10] M. Mishali and Y. C. Eldar, “Blind multiband signal reconstruction: Compressed sensing for analog signals,” *IEEE Transactions on signal processing*, vol. 57, no. 3, pp. 993–1009, 2009.
- [11] M. Mishali, Y. C. Eldar, and A. J. Elron, “Xampling: Signal acquisition and processing in union of subspaces,” *IEEE Transactions on Signal Processing*, vol. 59, no. 10, pp. 4719–4734, 2011.
- [12] P. Zhang *et al.*, “A compressed sensing based ultra-wideband communication system,” in *Communications, 2009. ICC’09. IEEE International Conference on*. IEEE, 2009, pp. 1–5.
- [13] K. Gedalyahu and Y. C. Eldar, “Time-delay estimation from low-rate samples: A union of subspaces approach,” *IEEE Transactions on Signal Processing*, vol. 58, no. 6, pp. 3017–3031, 2010.
- [14] K. Gedalyahu, R. Tur, and Y. C. Eldar, “Multichannel sampling of pulse streams at the rate of innovation,” *IEEE Transactions on Signal Processing*, vol. 59, no. 4, pp. 1491–1504, 2011.
- [15] N. Wagner, Y. C. Eldar, and Z. Friedman, “Compressed beamforming in ultrasound imaging,” *IEEE Transactions on Signal Processing*, vol. 60, no. 9, pp. 4643–4657, 2012.
- [16] T. Kazaz *et al.*, “Multiresolution time-of-arrival estimation from multiband radio channel measurements,” in *ICASSP 2019-2019 IEEE International Conference on Acoustics, Speech and Signal Processing (ICASSP)*. IEEE, 2019, pp. 4395–4399.
- [17] M. Viberg, B. Ottersten, and T. Kailath, “Detection and estimation in sensor arrays using weighted subspace fitting,” *IEEE transactions on Signal Processing*, vol. 39, no. 11, pp. 2436–2449, 1991.
- [18] A. L. Swindlehurst *et al.*, “Multiple invariance ESPRIT,” *IEEE Transactions on Signal Processing*, vol. 40, no. 4, pp. 867–881, 1992.
- [19] G. Golub and V. Pereyra, “Separable nonlinear least squares: the variable projection method and its applications,” *Inverse problems*, vol. 19, no. 2, p. R1, 2003.
- [20] R. Roy and T. Kailath, “ESPRIT-estimation of signal parameters via rotational invariance techniques,” *IEEE Transactions on acoustics, speech, and signal processing*, vol. 37, no. 7, pp. 984–995, 1989.
- [21] A. L. Swindlehurst, P. Stoica, and M. Jansson, “Exploiting arrays with multiple invariances using MUSIC and MODE,” *IEEE Transactions on Signal Processing*, vol. 49, no. 11, pp. 2511–2521, 2001.
- [22] A. F. Molisch *et al.*, “A comprehensive standardized model for ultrawideband propagation channels,” *IEEE Transactions on Antennas and Propagation*, vol. 54, no. 11, pp. 3151–3166, 2006.
- [23] T. Kazaz *et al.*, “Joint blind calibration and time-delay estimation for multiband ranging,” 2019, manuscript submitted for publication.
- [24] A.-J. Van Der Veen, E. F. Deprettere, and A. L. Swindlehurst, “Subspace-based signal analysis using singular value decomposition,” *Proceedings of the IEEE*, vol. 81, no. 9, pp. 1277–1308, 1993.